



A Novel Microwave Synthesis of Manganese Based MOF for Adsorptive of Cd(II), Pb(II) and Hg(II) Ions from Aqua Medium

H. M. Abd El Salam ^{1*} and T. Zaki ^{2,3}

¹Analysis and Evaluation Division, Egyptian Petroleum Research Institute, Nasr City, PO Box 11727, Cairo, Egypt.

²Catalysis Department, Petroleum Refining Division, Egyptian Petroleum Research Institute, Nasr City, PO Box 11727, Cairo, Egypt.

³EPRI-Nanotechnology Center, Egyptian Petroleum Research Institute, Nasr City, PO Box 11727, Cairo, Egypt.



THE manganese based MOF (Mn(BDC)(H₂O)₂); was successfully synthesized via a microwave method. The features of the Mn-MOF was evaluated by XRD, TGA, N₂ adsorption-desorption at -196°C, FTIR and SEM. The elimination of heavy metal ions from aqueous solution via Mn-MOF was described by batch adsorption tests including kinetic and thermodynamic models. Mn-MOF exhibited a very high adsorption efficiency towards Cd(II), Pb(II) and Hg(II) from aqueous solution (81.89%, 71.19% and 65.19% respectively). Adsorption kinetics data evidenced that heavy metal ions adsorption isotherms appropriated the Langmuir model and conform the pseudo-second-order kinetic equation. Successfully, the Mn-MOF was reused illustrative in the first run, the adsorbed amounts for (Cd(II), Pb(II) and Hg(II)) were (80.2%, 69.6% and 64%) after fifth run became (68%, 54.74% and 50.98% respectively) which is elucidating its potential for heavy metal ions decontamination application.

Keywords: Manganese-MOF, Cd(II), Pb(II), Hg(II), Adsorption; Interaction mechanism.

Introduction

Nowadays, the world is heading in thinking about removing heavy metals like Cd²⁺, Pb²⁺ and Hg²⁺ because of its hazard effects on the environment by its bio accumulative property as well as on human health cause kidney dysfunction, bone declination and blood deteriorate [1-8]. These ions have been emitted to the environment as a result of human activity through metal plating, mining activities, moulding, and battery fabricate industries [9-13]. Due to its toxicity, it was taken in the table of priority pollutants of (WHO). According to the list, the most lawful limit of Cd (II) is 0.005 ppm, and Hg (II) is 0.001 ppm in water [1, 14]. Various techniques have reported in the literature to remove these heavy metal ions from water, such as chemical precipitation, ion exchange, membrane filtration, and adsorption [15-17].

Adsorption process is now achieved as an operative and economic technique for heavy metal removal and displays cheap method, simple operating conditions, having wide pH zone and elasticity in functionality design [18-27]. Recently, metal-organic frameworks (MOFs), which are considered as new classes of microporous and mesoporous materials, have wide scientific attention due to their potential in an enormous range of applications in catalysis, separations, gas storage and sensing [28-30]. MOFs distinguishing very low density (0.2-1.5 g.cm⁻³), thermal stabilization and high surface area (500-5900 m².g⁻¹) [31-36]. So, it has been reported that MOFs have good adsorption capacity for the removal of pollutants such as dyes and hazardous metals.

Zheng and Richard reported the prepared of three known MOFs, sign to IRMOF1, IRMOF2,

*Corresponding author e-mail: howaida.abdelsalam@gmail.com

Received 6/12/2018; Accepted 1/1/2019

DOI: 10.21608/ejchem.2019.6524.1550

©2019 National Information and Documentation Center (NIDOC)

and IRMOF3, via a rapid microwave-assisted process [37]. Mn-MOF nanoparticles were synthesized solvothermally using Teflon-lined autoclave at high temperatures [38, 39]. Therefore, it is still stimulating to improve a simple, highly efficient and economical method for synthesizing Mn-MOF nanoparticles that can be used for adsorption of heavy metal ions like, Cd(II), Pb(II) and Hg(II) species. In this work, we successfully synthesized Mn-MOF using the microwave-assisted solvothermal method, which is a quick and operative way for preparing Mn-MOF, for a brief crystallization time. The adsorption behaviour of Mn-MOF towards heavy metals was monitored through a sequences of isotherm and kinetics experiments.

Experimental

Materials

Manganese (II) chloride ($\text{MnCl}_2 \cdot 4\text{H}_2\text{O}$, 99%), 1, 4-Benzenedicarboxylic acid ($\text{H}_2\text{BDC} \geq 98\%$), N, N-dimethylformamide ($\text{DMF} \geq 98\%$) and ethanol absolute ($\text{C}_2\text{H}_5\text{OH}$, 99.5%) were used without purification. Water used in all experiments was deionized.

Characterization

Thermogravimetric analysis (TGA, TA Instruments) was proceeded with a heating rate of $10^\circ\text{C}/\text{min}$ in a nitrogen flow. The powder XRD data which accomplished with a PAN analytical X'PERT PRO using $\text{CuK}\alpha$ X-ray radiation ($\lambda = 1.540 \text{ \AA}$) to investigate the crystal structure of the sample. The specific surface area and total pore volume were measured from the N_2 adsorption-desorption isotherms at (-196°C) using (Quantachrome NovaWin 3200) automatic gas sorption instruments. Before measurement, the sample was degassed at 150°C under vacuum. Fourier-transform infrared spectroscopy (FT-IR) spectrum of the sample was registered on Perkin Elmer (model spectrum one FT-IR spectrometer, USA) using KBr pellets over wave number range between 4000 and 500 cm^{-1} . The morphology structure of prepared sample was characterized by Scanning electron microscopy (SEM) Quanta 250 field emission gun (FEG) with an accelerating voltage of 30 kV .

Synthesis of Mn-MOF

H_2BDC (3.01 mmol) and $\text{MnCl}_2 \cdot 4\text{H}_2\text{O}$ (5.20 mmol) were dissolved in the mixture of DMF, ethanol, and deionized water in a volume ratio (1:1:1) under vigorous stirring at room temperature. Subsequently, the resultant was transferred to a round glass bottle connected with a

reflux condenser and placed in microwave heated at 300 watts for 240 min . The resulting product was centrifuged, washed several times with DMF and then washed with methanol. Finally, the as-synthesized sample was dried at 100°C for 10 hrs .

Adsorption experiments

Stock solution (1000 mg/L) of heavy metal ions prepared by dissolving the necessary amount of $\text{Cd}(\text{NO}_3)_2 \cdot 4\text{H}_2\text{O}$, $\text{Pb}(\text{NO}_3)_2$ and HgCl_2 in distilled water. For studying the adsorption isotherm, thermodynamic models, and kinetics of the adsorption process, the experiments were achieved at diverse concentrations ($25, 50, 100, 150$ and 250 mg/l) and temperatures ($20, 30, 40$ and 50°C) using different adsorbent amount of Mn-MOF ($10, 25, 50$, and 100 mg). The agitation times were ($1, 2, 4, 6, 12, 18$ and 24 h). The pH values were adjusted to ($1, 3, 5, 6$ and 7) using 0.1 M NaOH or HCl solution. All adsorption evaluations were achieved in bottles and softly agitated on a temperature regulated water-bath shaker at 250 rpm . At the end of every adsorption test, the solids were filtered through a centrifuge. After that, the supernatant was obtained and analyzed for the Cd, Pb and Hg concentrations by atomic absorption spectrometry (CVAAS) ZEE nit 700P Analytik Jena (Germany). The metal removal percentage was estimated using Equation (1) where (C_0 and C_e) represent the initial and equilibrium metal ion concentrations mg/L respectively.

$$\text{Metal Removal \%} = \left(\frac{C_0 - C_e}{C_0} \right) \times 100 \text{ (Eq. 1)}$$

Results and Discussion

Characterization of Mn-MOF

The thermogravimetric analysis (TGA) curves exhibited three weight loss steps (Fig. 1). The first weight loss ($\sim 15 \text{ wt \%}$) over the temperature ranging from 35°C to 200°C , it corresponded to the loss of physisorbed water molecules in the pores of Mn-MOF. The second weight loss ($\sim 35 \text{ wt \%}$) at 550°C and was corresponded to disintegrate the metal-organic structure [40]. The third weight loss ($\sim 19 \text{ wt \%}$) around the temperature 550°C to 800°C which can be attributed to complete transformation into MnO [41]. The prepared sample showed thermal stability higher than the previously published work [40], which may be resulted from fast crystallization under the microwave irradiation. The X-ray diffraction pattern of the synthesized Mn-MOF (Fig. 2), showed the diffraction peaks at $9.3^\circ, 14.1^\circ, 18.5^\circ, 19.1^\circ, 24.2^\circ$,

28.1°, 29.3°, and 34.3° are significantly agreement with the previously published literature [38, 41] and confirmed the successful synthesis under the microwave-assisted solvothermal method with high crystalline. The Fourier transform infrared (FTIR) spectrum of as-synthesized Mn-MOF (Fig. 3) showing the stretching vibrations at ~3450

and ~3114 cm^{-1} clarified the existence of the coordinated water molecules in the structure of Mn-MOF [42-44] and the specification of two peaks at 1587 and 1385 cm^{-1} corresponds to the symmetric and asymmetric stretching of the coordinated carboxylate (COO-Mn) [42-45]. In addition, band appeared at ~1740 cm^{-1} which attributed to C=C-C

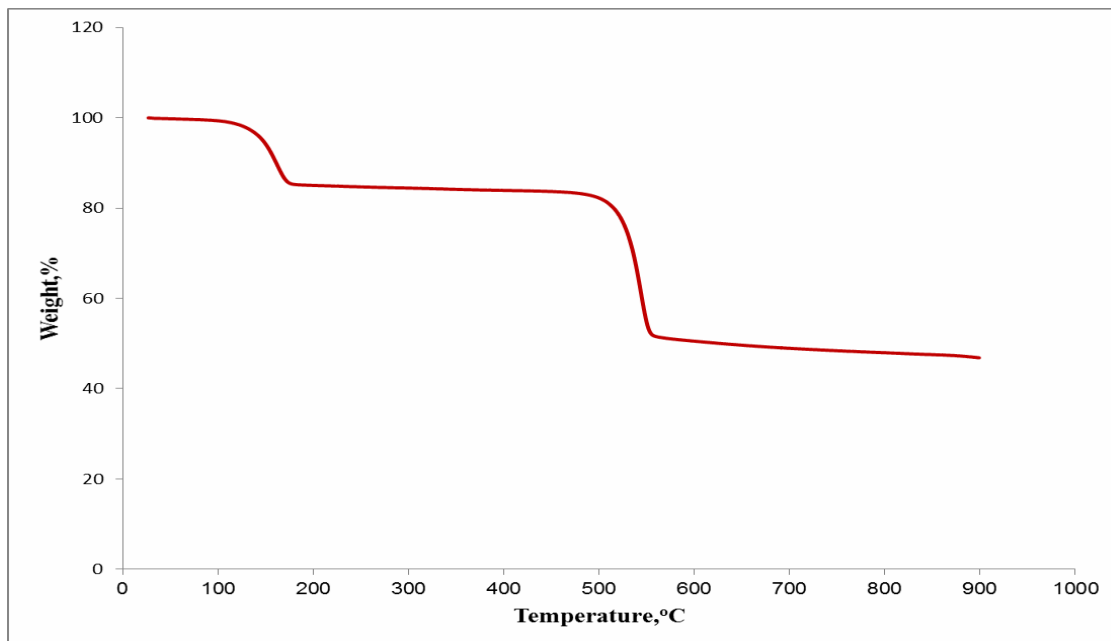


Fig. 1. TGA analysis of Mn-MOF sample was proceeded with a heating rate of 10°C /min in a nitrogen flow.

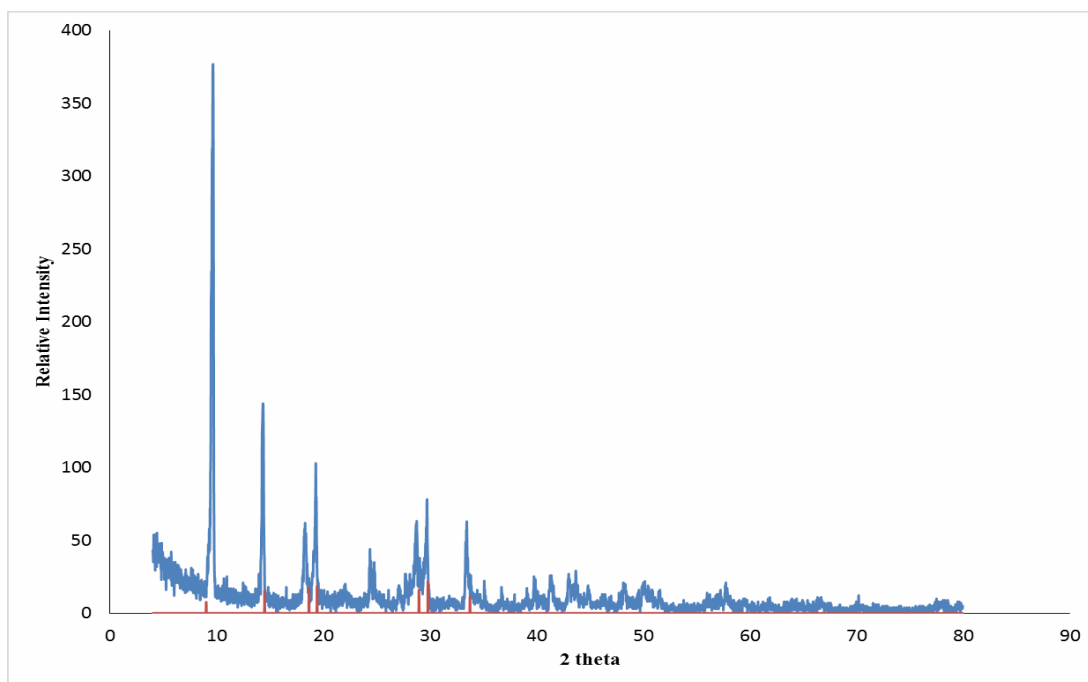


Fig. 2. XRD pattern of synthesized Mn-MOF using the microwave-assisted solvothermal method.

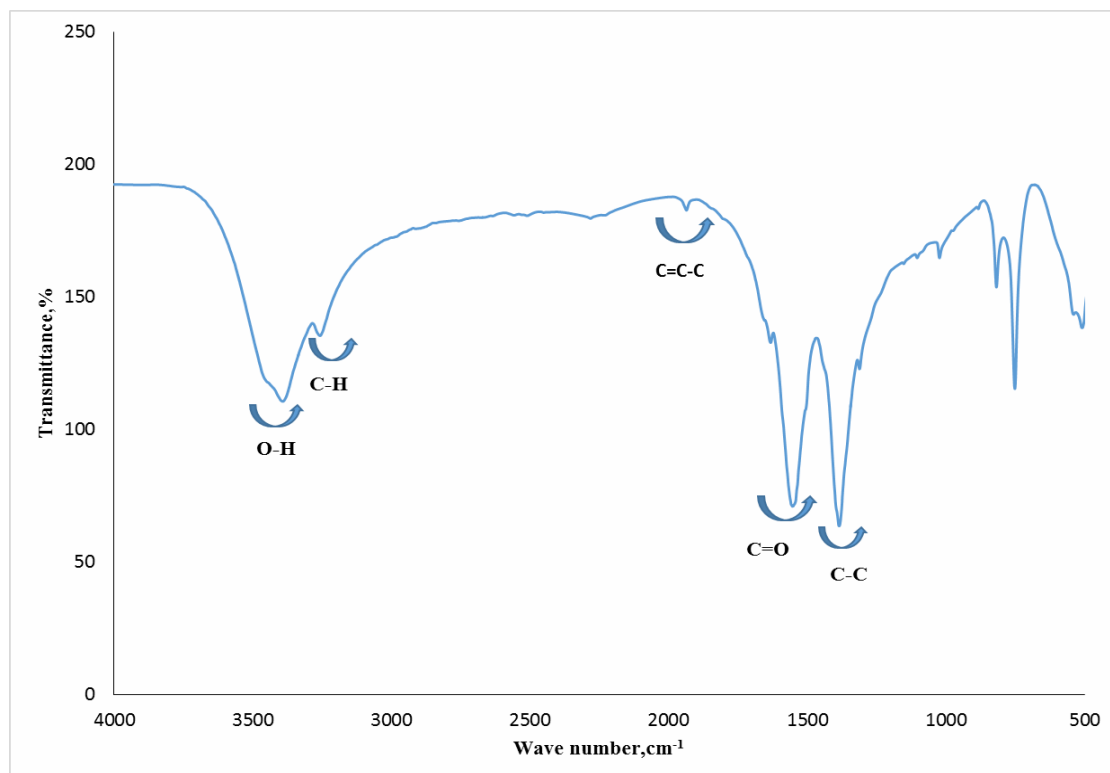


Fig. 3. FT-IR Spectra of synthesized Mn-MOF sample.

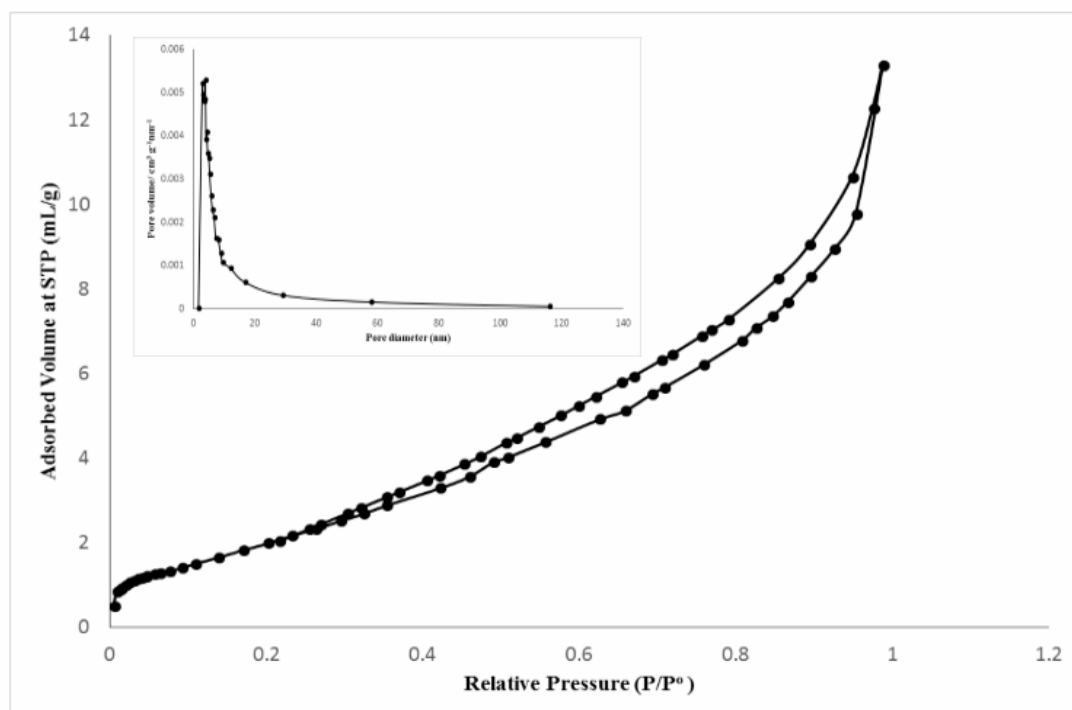


Fig. 4. Nitrogen adsorption-desorption isotherms and BJH desorption pore size distributions of as-synthesized Mn-MOF. *Egypt.J.Chem.* 62, No. 5 (2019)

TABLE 1. Surface features of the prepared Mn-MOF.

Sample code	S_{BET} (m^2/g)	V_p (cm^3/g)	r_H (nm)
Mn-MOF	8.91	0.02	46.13

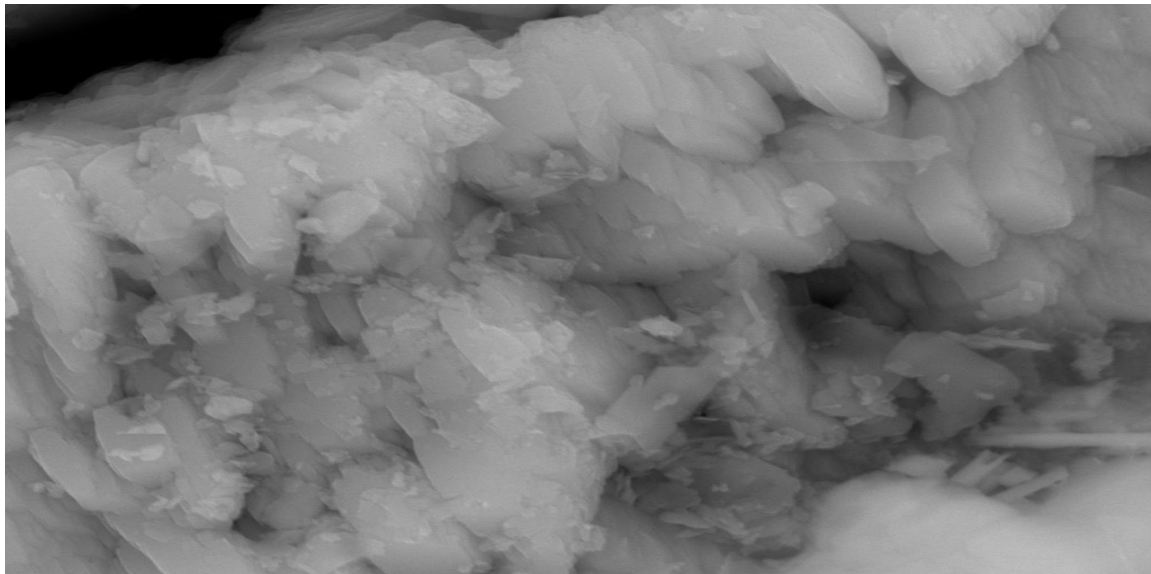


Fig. 5. SEM micrographs of as-synthesized Mn-MOF sample.

[30]. Also, the spectrum showed several small peaks occurring in the range of $1250\text{--}1010\text{ cm}^{-1}$, which identified with the C–H group present in the benzene ring of the benzenedicarboxylic linker. The Nitrogen adsorption–desorption isotherm of Mn-MOF sample showed type IV isotherm for mesoporous materials (Fig. 4). Surface features (Table 1) clarified comparable surface area ($\sim 8.91\text{ m}^2/\text{g}$) with the previously published Mn(BDC) MOFs [40, 46]. The SEM image of Mn-MOF showed the morphology of bulky laminar structure aggregates (Fig. 5).

Adsorption activity

Influence of contact time and adsorption kinetics

The results (Fig. 6) showed that the adsorption rate of (Cd(II), pb(II) and Hg(II)) increased sharply after the first 1h to reach 39.8%, 25.17% and 20.34% respectively, which may be the presence of a great number of available adsorption surface sites. A number of metal ions adsorbed is affected by the velocity by which the adsorbates, which were delivered from the external to the internal of active sites of the adsorbent surfaces. The highest activity of the adsorption metal ions was achieved after 6h to reach 81.89% for Cd(II), 71.19% for pb(II) and 65.19% for Hg(II) ($\text{Cd} > \text{pb} > \text{Hg}$) and then it reaches the equilibrium

after 12h. The removal efficiency towards metals is varied as a result electronegativity, when the greater difference in electronegativity between two atoms the more polar the bond that will be formed between them [47].

Adsorption kinetics were used to evaluate the mechanism adsorptive of heavy metal ions on Mn-MOF as a perform of the time and the results are illustrated in Fig. 7a, b. The pseudo-first-order and second-order equations (equations 2 and 3) were applied to analyze the experimental data were given as.

$$\ln(q_e - q_t) = \ln(q_e) - \left(\frac{K_1}{2.303}\right)t. \quad (\text{Eq.2})$$

$$\frac{t}{qt} = \frac{1}{K_2 q_e^2} + \frac{t}{q_e}. \quad (\text{Eq.3})$$

Where (q_e and q_t) mg g^{-1} are the amount of adsorbate heavy metals at balance and at time (t), respectively. (K_1 and K_2) are the rates stationary of pseudo-first-order and second-order for the adsorption mechanism. The values of q_e and K are specified in Table 2. Based on the values of the correlation coefficients (R^2), which were about 0.99, the pseudo-second order model can be applied to describe the adsorption of metal ions by Mn-MOF

better than pseudo-first order model. Furthermore, q_e (exp.) and q_e (calc.) rates were close to each other.

Adsorption isotherms

To appreciate the adsorption capacity of synthesis Mn-MOF towards the reducing of metal ions from aqua media at a various concentration from 25 - 250 mg/l. The data are given in Fig. 8. It shows that the adsorption activity of Cd^{2+} , Pb^{2+} , and Hg^{2+} decreases gradually with the increasing concentration of metal ions until there occurs a maximum absorption, it is attributed to lack of active sites to receive more ions available in the solution. The adsorption parameters can be determined by transforming the Langmuir (Eq.

4) and Freundlich (Eq. 5) isotherms, which were plotted to appropriate the experimental data by employ equations of standard straight-line:

$$\frac{1}{q_e} = \frac{1}{C_e q_m k_L} + \frac{1}{q_m} \quad (\text{Eq.4})$$

$$\ln(q_e) = \ln(k_F) + \frac{1}{n} \ln(C_e) \quad (\text{Eq.5})$$

where C_e (ppm) is the concentration of the solute at equilibrium, q_e ($mg\ g^{-1}$) is the amount of solution adsorbed per unit mass, q_m is the most adsorption intensity ($mg\ g^{-1}$), and k_L ($L\ mg^{-1}$) is the Langmuir

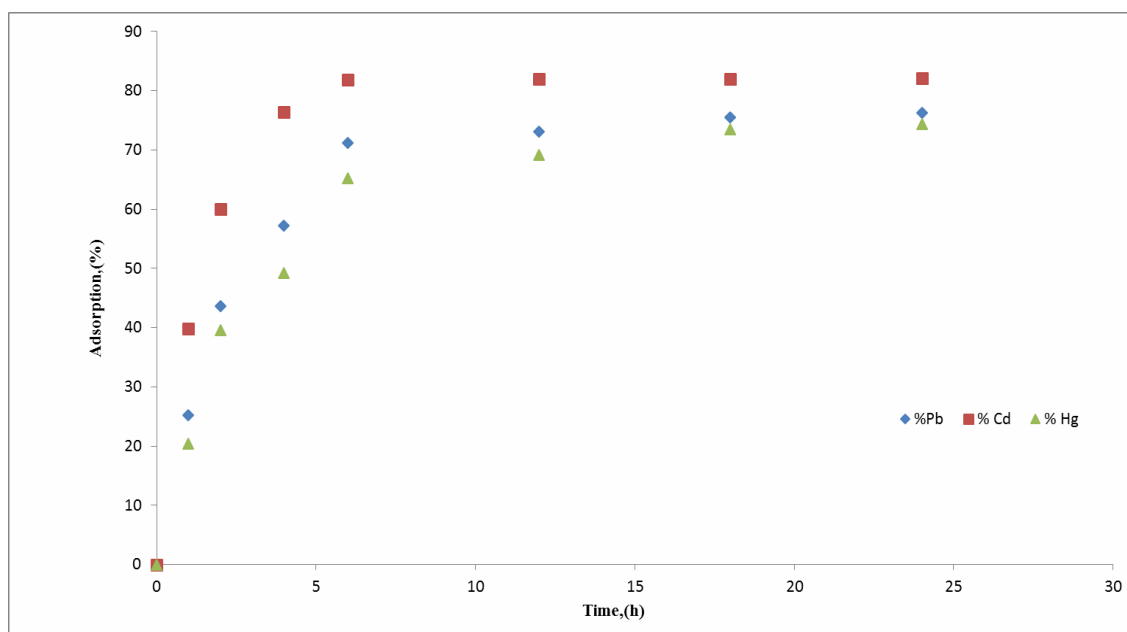


Fig. 6. Influence of contact time on the adsorption behavior of heavy metal ions by Mn-MOF (50 mg adsorbent, 50 ppm Stock solution of heavy metal ions, 30°C, pH 5).

TABLE 2. Kinetic parameters for heavy metal ions adsorption on the prepared sample Mn-MOF.

Heavy metals	$q_{e,exp}$ (mg/g)	Pseudo-first-order model			Pseudo-second-order model		
		q_e (mg/g)	k_1 (min^{-1})	R^2	q_e (mg/g)	k_2 ($g \cdot mg^{-1} \cdot min^{-1}$)	R^2
Cd(II)	63.62	53.83	0.00230	0.8950	58.83	0.00075	0.998
Pb(II)	57.55	53.81	0.00230	0.9710	54.33	0.00031	0.994
Hg(II)	52.67	49.54	0.00221	0.9690	50.74	0.00024	0.990

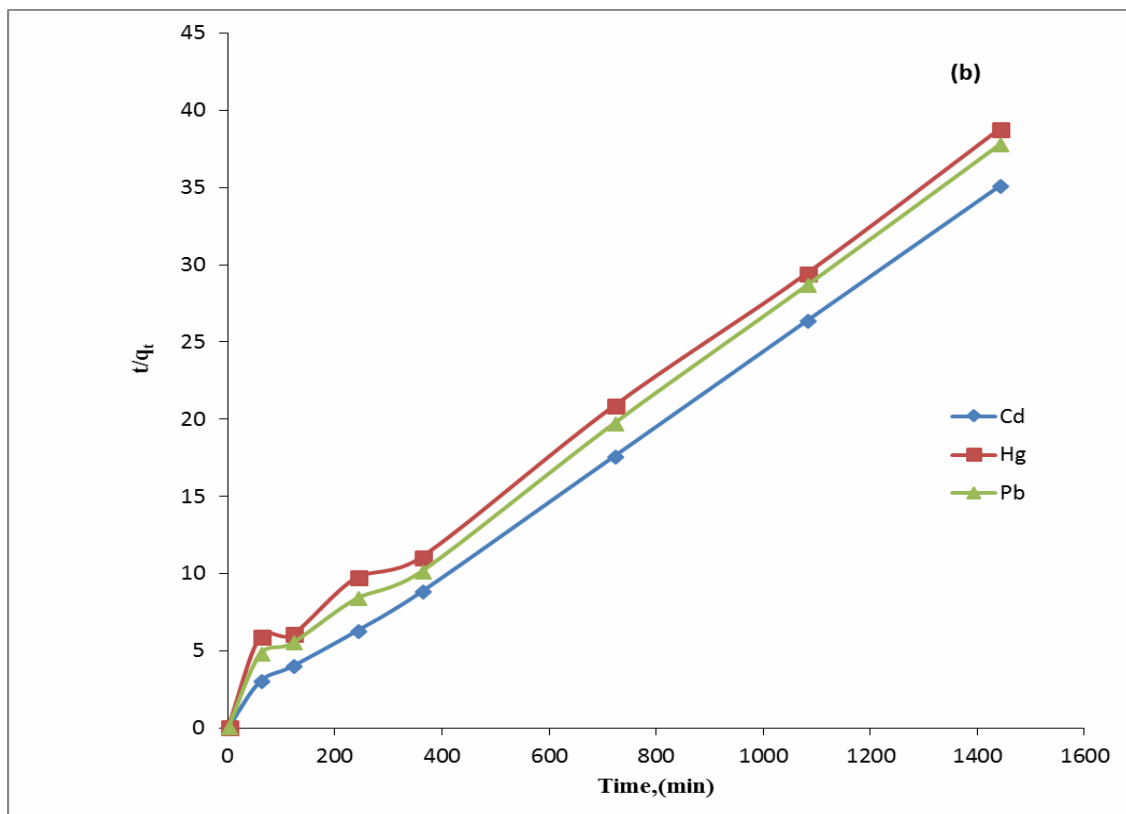
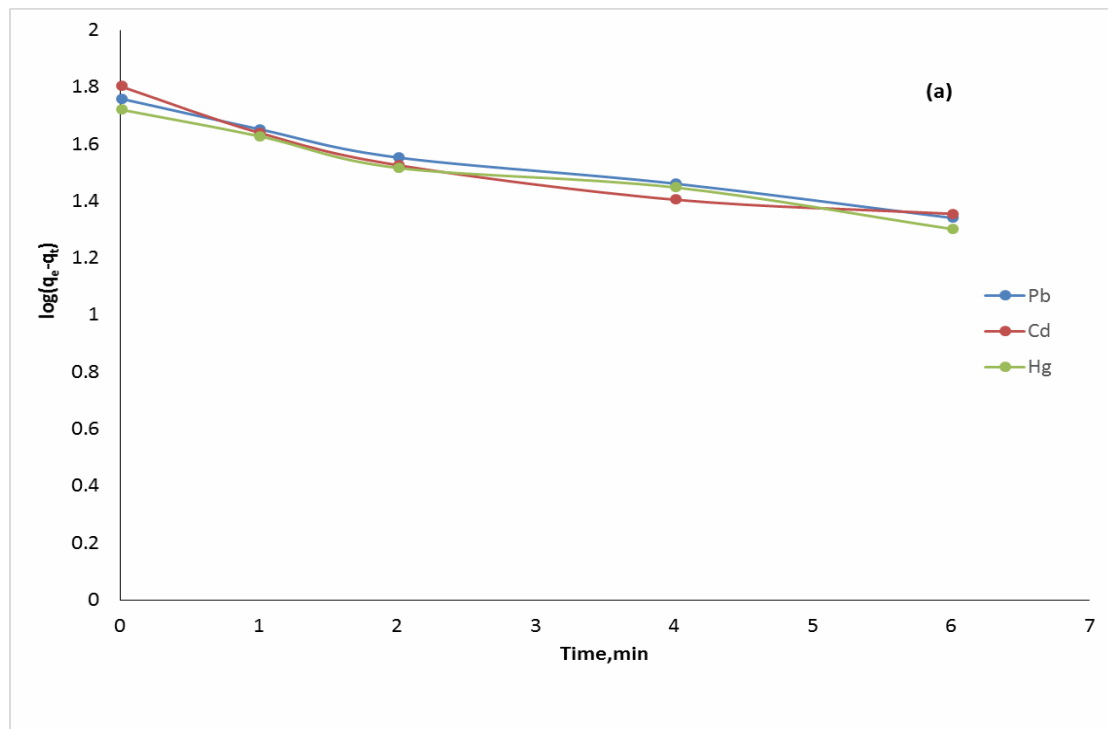


Fig. 7(a, b). Adsorption kinetics for heavy metal ions removal by Mn-MOF.

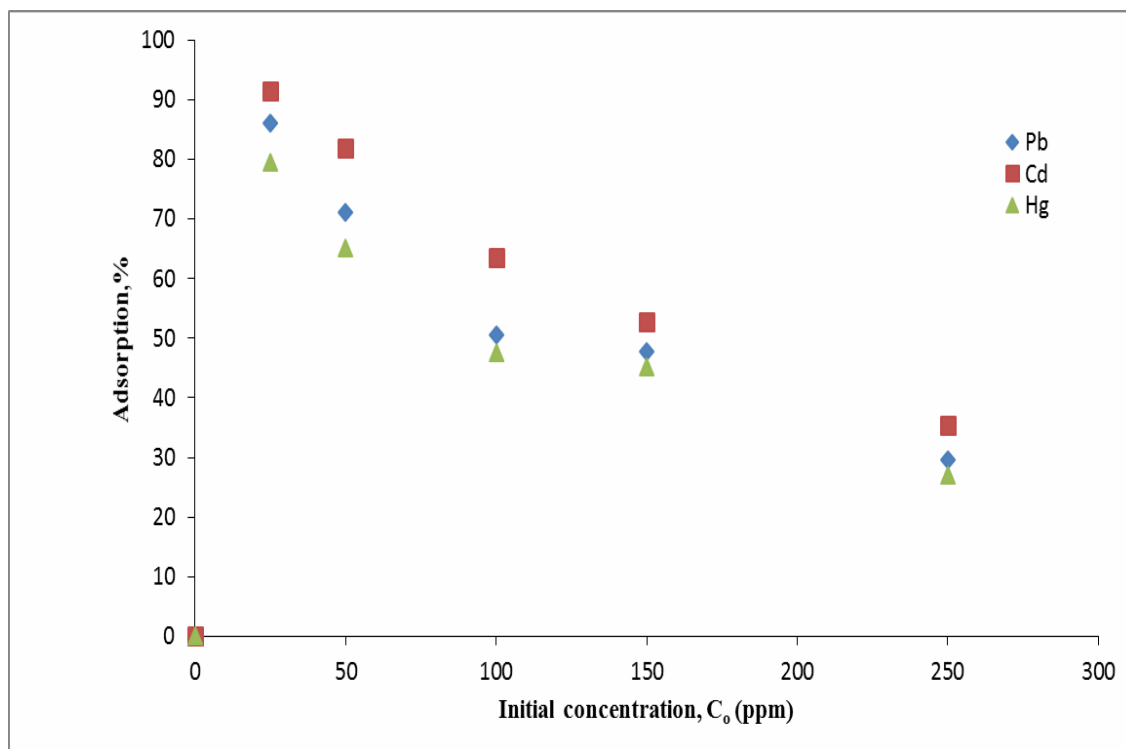


Fig. 8. Influence of adsorbate concentration on the adsorption behavior of heavy metal ions by Mn-MOF (50 mg adsorbent, 360 min, 30°C, pH 5).

TABLE 3. Adsorption isotherm parameters for heavy metal ions adsorption on the prepared sample Mn-MOF.

Heavy metals	Adsorption isotherms						
	Langmuir equation				Freundlich equation		
	q_m (mg/g)	k_L (L.mg ⁻¹)	R^2	R_L	K_F (mg.g ⁻¹)	1/n	R^2
Cd(II)	131.58	21.32	0.9900	0.9420	178.6	0.759	0.7030
Pb(II)	104.17	15.54	0.9770	0.9332	175.5	0.731	0.6940
Hg(II)	96.15	7.91	0.9670	0.9589	167.6	0.720	0.7000

constant. k_F (mg^{-1/n} L^{-1/n} g⁻¹) and n are the Freundlich constants relative to the adsorption efficiency and adsorption concentration. The results of modeling are listed in Table 3. According to the correlation coefficient r^2 values, the Langmuir model can describe the experimental data better than Freundlich model. The R_L values, which were 0.9000 indicated the favorability of the adsorption process [48]. The Langmuir model which can be applied for homogenous surfaces and monolayer

Egypt.J.Chem. **62**, No. 5 (2019)

adsorption and there are no interactions between adsorbed species [49].

Influence of adsorbent dosage

The impact of Mn-MOF dose on the adsorptive of heavy metal ions was shown in Fig. 9. Metal ions uptake efficiency increased quickly with the increasing dosage of adsorbent from 0.01 to 0.1 g/L, metal ions concentration of 50 mg/l and a fixed agitation speed (200 rpm). In this period, with increasing adsorbent dosage

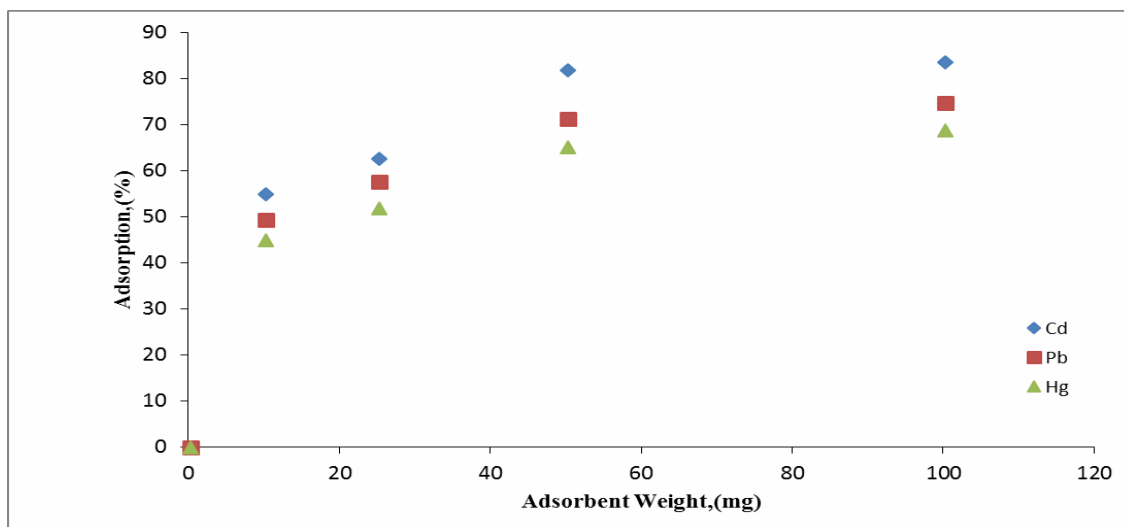


Fig. 9. Influence of adsorbent dose (mg) on the adsorption behavior of heavy metal ions by Mn-MOF (50 ppm Stock solution of heavy metal ions, 360 min, 30°C, pH 5).

more surface area and more active sites were great available for adsorption, thus more heavy metal ions could be removed. This result can be due to the adsorption sites keep unsaturated through the adsorption reaction but eventually increase with increasing concentration of adsorbent. However, the uptake of the metal ions was observed to be (54.92%, 49.38% and 44.90%) for Cd(II), pb(II) and Hg(II), respectively at the adsorbent concentration of 0.01 g L⁻¹ and increased to

be (81.89%, 71.19% and 65.19%) at adsorbent concentration of 0.05 g.

Influence of pH

The solution pH is a dynamic parameter in the adsorption method because it can convert the charge of adsorbent surface. The adsorption of heavy metal ions on synthesis Mn-MOF is greatly influenced by the initial pH (Fig. 10). The maximum (Cd(II), pb(II) and Hg(II)) removal

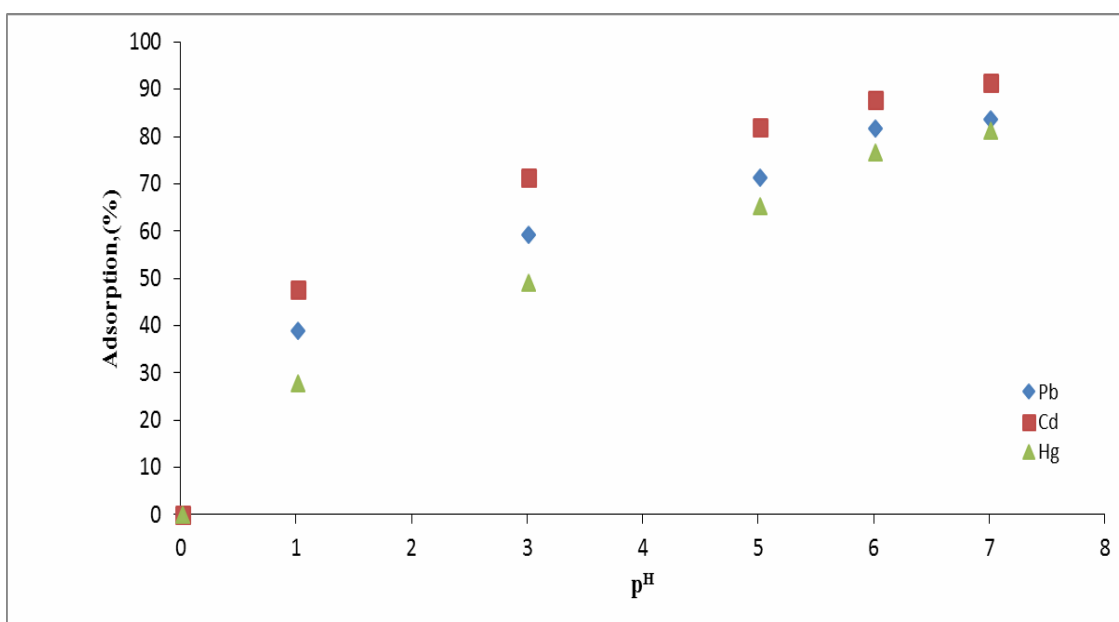
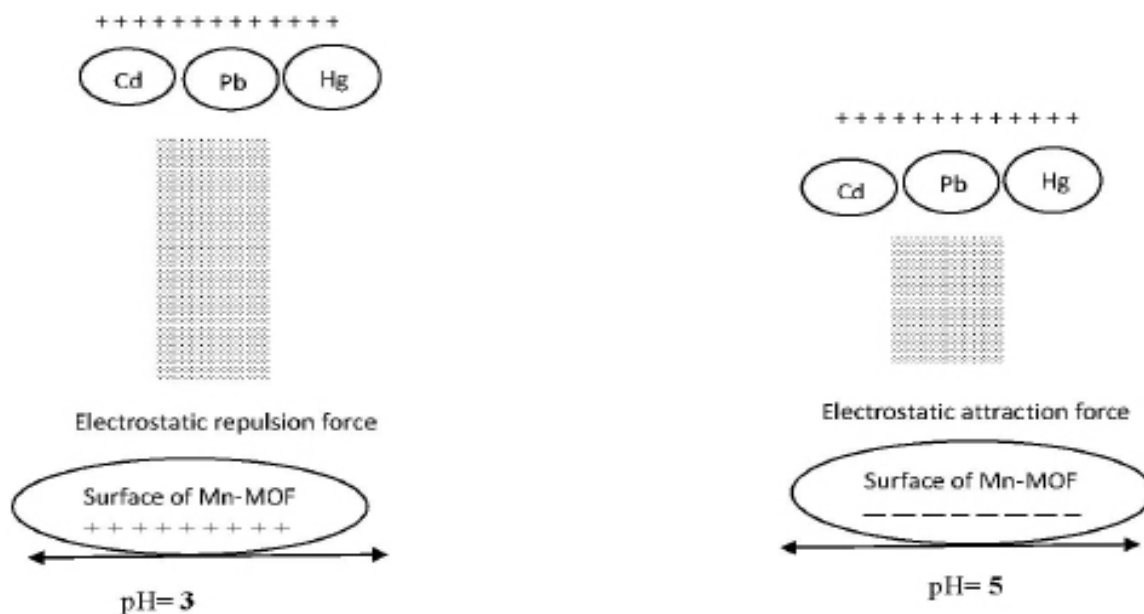


Fig. 10. Influence of pH values on the adsorption behavior of heavy metal ions by Mn-MOF (50 mg adsorbent, 50 ppm Stock solution of heavy metal ions, 30°C, 360 min).



Mechanism of heavy metal ions removal on surface of Mn-MOF at varied pH .

efficiency on Mn-MOF was about (81.72%, 71.71% and 68.69%), respectively at pH5. At lower pH values heavy metal ions removal were restrained, probably the repulsive force between positive surface and metal ions. As the pH increased, increasing the concentration of negative charge on the adsorbed surface, increasing the force attractive of metal ions with positive charge. pH values ≥ 6 , the precipitation of metal occurred and efficiency of adsorbent was decreased with aggregation of metal ions. Therefore, an optimum pH 5.0 was preferable for furthermore experiments.

Adsorption thermodynamics

Thermodynamic analysis was performed to illustrate the eventuality of heavy metal ions adsorption onto Mn-MOF at different temperatures (20-50°C). Changes of free energy (ΔG°), enthalpy (ΔH°) and entropy (ΔS°) were evaluated according to the following equations (Eq.6, 7):

$$\Delta G^\circ = -RT \ln K_c \quad (\text{Eq.6})$$

$$\Delta G^\circ = \Delta H^\circ - T\Delta S^\circ \quad (\text{Eq.7})$$

Figure 11 shows that the elimination percentage increases with increasing the temperature. According to the results (Table 4), (-ve) values of ΔG° elucidate the spontaneous behavior of the adsorption process, which does not require an

extrinsic energy. The decrease in ΔG° with the increase of temperature implies more effective adsorption at higher temperature. The (+ve) ΔH° values emphasize the endothermic nature of the adsorption, which explains the increase of heavy metal ions adsorption performance as the temperature increased. The positive value for ΔS° , signalizes that there is an increased disorder at the solid solution interface during metal ions adsorption onto the Mn-MOF.

Desorption

The regeneration of adsorbent material for heavy metal ions removal are important aspects of studies, because they can reduce the cost of operation and will be more economical. In this study, the used Mn-MOF was regenerated by washing with acetone several times. The performances of the regenerated Mn-MOF was a little low compared to the fresh Mn-MOF; however, the adsorbed amounts for Cd(II), Pb(II) and Hg(II) did not change after the fifth run (Fig. 12), suggesting the stability of Mn-MOF as an adsorbent.

Conclusion

Mn-MOF with high purity and crystallinity was successfully synthesized by the microwave-assisted solvothermal method. Mn-MOF showed high adsorption capacities for heavy metal ions from aqueous medium. Adsorption kinetics

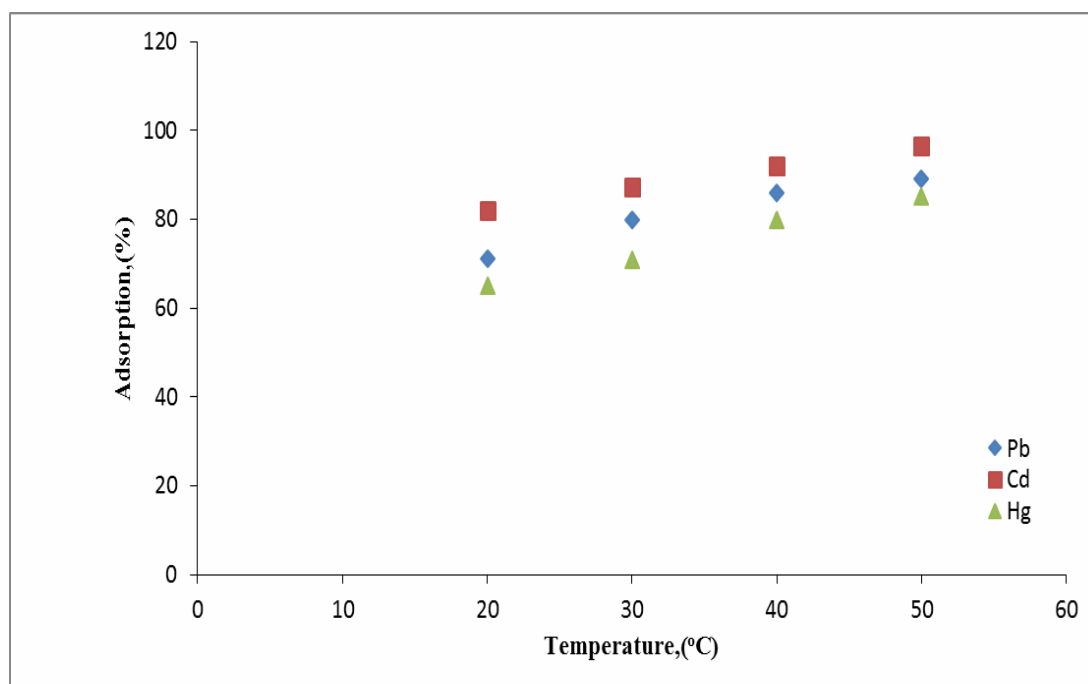


Fig. 11. Influence of temperature on the adsorption behavior of heavy metal ions by Mn-MOF (50 mg adsorbent, 50 ppm Stock solution of heavy metal ions, 360 min, pH 5).

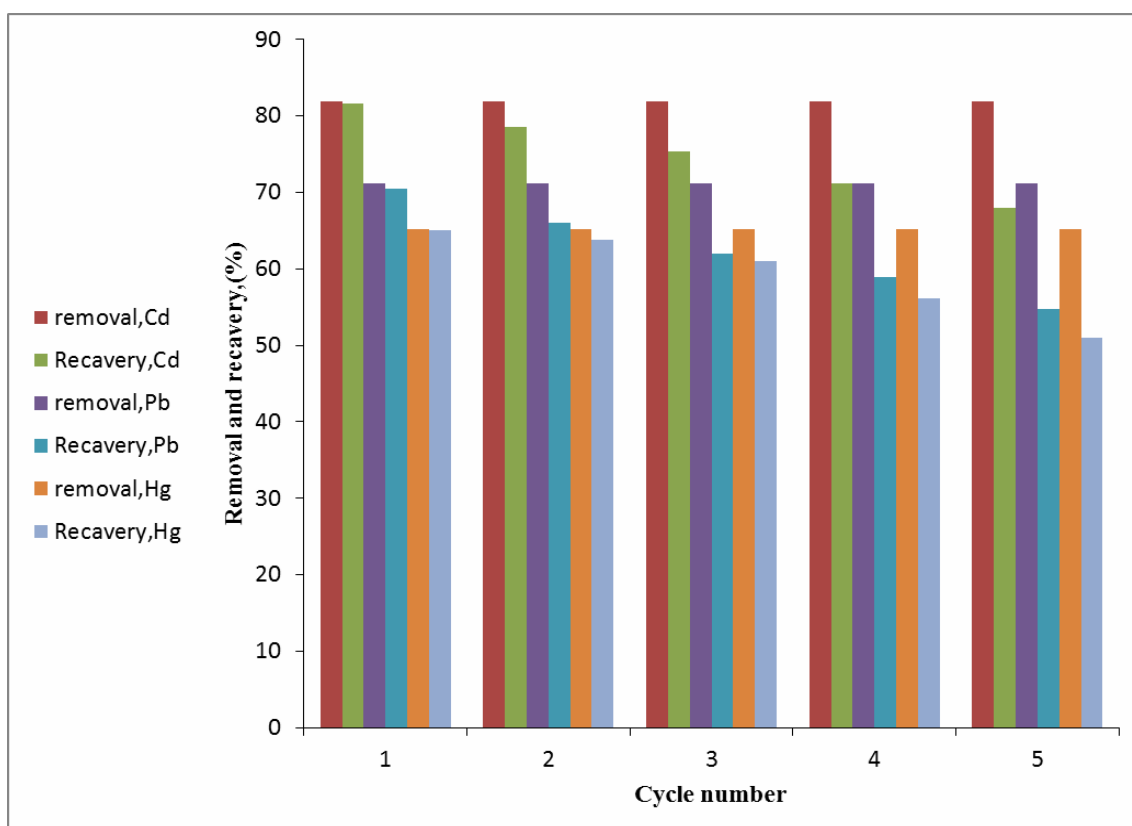


Fig. 12. Reusability of The Mn-MOF.

TABLE 4. Thermodynamic parameters for heavy metal ions adsorption on the prepared sample Mn-MOF.

Heavy metals	ΔG° (kJ.mol ⁻¹) at different T (K)				ΔS° (J.mol ⁻¹)	ΔH° (kJ.mol ⁻¹)
	293	303	313	323		
Cd(II)	-3.7	-4.9	-6.3	-8.8	0.1677	45.75
Pb(II)	-2.2	-3.5	-4.7	-5.6	0.1154	31.55
Hg(II)	-1.5	-2.3	-3.6	-4.3	0.1070	29.95

data, revealed that (Cd(II), pb(II) and Hg(II)) adsorption isotherms favorable the Langmuir model and conform the pseudo-second order kinetics equation. The removal percentage of these ions by Mn-MOF increases by increasing the temperature of solution, it means that adsorption is endothermic. The maximum removal efficiency of (Cd(II), pb(II) and Hg(II)) ion by Mn-MOF is at pH= 5. Regeneration process elucidative that, the possibility of reusing Mn-MOF several times where the adsorbed amounts for (Cd(II), pb(II) and Hg(II)) were (80.2%, 69.6% and 64%)In the first run, after fifth run became (68%, 54.74% and 50.98% respectively).

References

- Rao K. S., Anand S., Warlue P. V., Adsorption of cadmium (II) ions from aqueous solution by Tectonagrandis L.F. (teak leaves powder), *Bio Resources* **5**(1), 438-454 (2010).
- Lehoczky E., Szabo L., Horvath Sz., Marth p., Szabados I., Cadmium uptake lettuce in different soils, *Commun. Soil Sci. Plant. Anal.* **29** (11-14), 1903-1912 (1998).
- Kuban P., Hauser P.C., Kuban V., Mercury Speciation by CE: A Review, *Electrophoresis* **28**, 58-68 (2007).
- Oehmen A., Viegas R., Velizarov S., Reis M. A.M., Crespo J. G., Removal of heavy metals from drinking water supplies through the ion exchange membrane bioreactor, *Desalination* **199**, 405-407 (2006).
- Zheng Y., Jensen A.D., Windelin C., Jensen F., Review of technologies for mercury removal from flue gas from cement production processes, *Progress in Energy and Combustion Science* **38**, 599-629 (2012).
- Xu W., Wang H., Zhu T., Kuang J., Jing P., Mercury removal from coal combustion flue gas by modified fly ash, *Environ. Sci. (China)* **25**, 393-398 (2013).
- Alshabanat M., Removal of heavy metal ions using polystyrene nanocomposite thin films, *Egyptian J. of Chemistry*, **62**, 16-17 (2019).
- El-Shamy A. M., Farag H. K., Saad W., Comparative Study of Removal of Heavy Metals from Industrial Wastewater Using Clay and Activated Carbon in Batch and Continuous Flow Systems, *Egyptian J. of Chemistry*, **60**, 1165-1175 (2017).
- Putra W. P., Kamari1A., Yusoff S. N. M., FauziahIshak C., Mohamed A., Hashim N., Isa I. Md, Bio sorption of Cu(II), Pb(II) and Zn(II) Ions from Aqueous Solutions Using Selected Waste Materials, *Adsorption and Characterization Studies, Encapsulation and Adsorption Sciences* **4**, 25-35 (2014).
- Erto A., Giraldo L., Lancia A., Moreno-Pirajan J. C., A Comparison between a Low-Cost Sorbent and an Activated Carbon for the Adsorption of Heavy Metals from Water, *Water, Air, & Soil Pollution* **224**, 1-10 (2013).
- Ibrahim M. N., Wan Ngah W. S., Norliyana M. S., Daud W. R., Rafatullah M., Sulaiman O., A Novel Agricultural Waste Adsorbent for the Removal of Lead (II) Ions from Aqueous Solutions, *Hazardous Materials* **182**, 377-385 (2010).
- Owamah H. I., Bio sorptive Removal of Pb(II) and Cu(II) from Wastewater Using Activated Carbon from Cassava peels, *Material Cycles and Waste Management* 1-12 (2013).
- Spiro T.G., Stagliani, T.G., *Chem. of the Environ.* Prentice Hall, NewYork, (1996).
- Zhang F. S., Nriagu J. O., Itoh H., Mercury removal from water using activated carbons

- derived from organic sewage sludge, *Water Res.* **39**, 389 (2005).
15. Fu F., Wang Q., Removal of Heavy Metal Ions from Wastewaters: A Review. *Environmental Management* **92**, 407-418 (2011).
 16. Lloyd-Jones P. J., Rangel-Mendez J. R., Streat M., Mercury Sorption from Aqueous Solution by Chelating Ion Exchange Resins, Activated Carbon and a Biosorbent, *Process Safety and Environ. Protection* **82**, 301–311 (2004).
 17. Wang Z., Abraham R., Sulfur-impregnated organo-clay mercury and/or arsenic ion removal media, USPTO patent application 20080302730, May (2008).
 18. Pan B. J., Pan B. C., Zhang W. M., Lv L., Zhang Q. X., Zheng S. R., Development of polymeric and polymer-based hybrid adsorbents for pollutants removal from waters, *J. Chem. Eng.* **151**, 19 (2009).
 19. Mishra S. P., Singh V. K., Tiwari D., Radiotracer technique in adsorption study. 14. Efficient removal of mercury from aqueous solutions by hydrous zirconium oxide, *Appl. Radiat. Isot.* **47**, 15 (1996).
 20. Hua M., Zhang S., Pan B., Zhang W., Lv L., Zhang Q., Heavy metal removal from water/wastewater by nanosized metal oxides: A review, *Hazard. Mater.* **211**, 317 (2012).
 21. Benguella B., Benaissa H., Cadmium removal from aqueous solutions by chitin: kinetic and equilibrium studies, *Water Res.* **36**, 2463-2474 (2002).
 22. Gomez-Salazar S., Lee J. S., Heywieller J. C., Tavlarides L. L., Analysis of cadmium adsorption on novel organo-ceramic adsorbents with a thiol functionality, *Ind. Eng. Chem. Res.* **42**, 3403-3412 (2003).
 23. Singh K. K., Rastogi R., Hasan S. H., Removal of cadmium from waste water using agricultural waste rush polish, *Hazard. Mater.* **121**, 51-58 (2005).
 24. Nwabanne J. T., Ibbokwe P. K., Kinetics and equilibrium modeling of nickel adsorption by cassava peel, *Eng. Applied Sci.* **3**, 829-834 (2008).
 25. Hadi P., To M. H., Hui C. W., Lin C. S. K., McKay G., Review Aqueous mercury adsorption by activated carbons, *Water Research* **73**, 37-55 (2015).
 26. Hadi P., Barford J., McKay G., Selective toxic metal uptake using an e-waste-based novel sorbente Single, binary and ternary systems, *Environ. Chem. Eng.* **2**, 332-339 (2014).
 27. Anirudhan T.S., Shainy F., Effective removal of mercury(II) ions from chlor-alkali industrial wastewater using 2-mercaptobenzamide modified itaconic acid-grafted-magnetite nanocellulose composite, *Journal of Colloid and Interface Science* **456**, 22–31 (2015).
 28. O'Keeffe M., Yaghi O.M., Review Deconstructing the Crystal Structures of Metal–Organic Frameworks and Related Materials into Their Underlying Nets, *Chem. Rev.* **112**, 675–702 (2012).
 29. Abd El Salam H.M., Younis S.A., Ali H.R., Zaki T., Statistical modeling and optimization of phenol adsorption from water by modified Cu₃(BTC)₂: Kinetic, isotherm, and thermodynamic analysis, *Microporous and Mesoporous Materials* **241**, 210-217 (2017).
 30. Abd El Salam H.M., Zaki T., Removal of hazardous cationic organic dyes from water using nickel based metal-organic frameworks, *Inorganica Chimica Acta* **471**, 203–210 (2018).
 31. Küssgens P., Rose M., Senkovska I., Fröde H., Henschel A., Siegle S., Kaskel S., Characterization of metal-organic frameworks by water adsorption, *Microporous and Mesoporous Materials* **120**, 325–330 (2009).
 32. Kaskel S., Schüth F., Sing K.S.W., Weitkamp J., *Handbook of Porous Solids*, Wiley VCH, Weinheim, 1190 (2002).
 33. Yaghi O.M., Li H.L., Davis C., Richardson D., Groy T.L., Synthetic Strategies, Structure Patterns, and Emerging Properties in the Chemistry of Modular Porous Solids, *Acc. Chem. Res.* **31**, 474-484 (1998).
 34. Eddaoudi M., Kim J., Rosi N., Vodak D., Wachter J., O'Keefe M., Yaghi O.M., Systematic design of pore size and functionality in isorecticular MOFs and their application in methane storage, *Science* **295**, 469–472 (2002).
 35. Jhung S.H., Khan N. A., Hasan Z., Analogous porous metal organic frameworks: Synthesis, stability and application in adsorption, *Cryst. Eng. Comm.* **14**, 7099-7109 (2012).
 36. Wu H., Gong Q., Olson D.H., Li J., Commensurate adsorption of hydrocarbons and alcohols in

- microporous metal organic frameworks, *Chem. Rev.* **112**, 836-868 (2012).
37. Zheng N., Richard M. I., Rapid Production of Metal-Organic Frameworks via Microwave-Assisted Solvothermal Synthesis, *J. Am. Chem. Soc.* **128**, 12394-12395 (2006).
38. Ranjbar M., Taher M. A., A. Sam, Facile hydrothermal synthesis of manganese-metal organic framework nanostructures in the presence of various organic ligands for SO₂ and CO₂ gas adsorption, *Porous Mater.*, 375-380 (2016).
39. Peng L., Zhang J., Xue Z., Han B., Li J., Yang G., Large-pore mesoporous Mn₃O₄ crystals derived from metal organic frameworks, *Electronic Supplementary Material (ESI) for Chemical Communications* (2013).
40. Hu H., Lou X., Li Ch., Hu X., Li T., Chen Q., Shen M., Hu B., A thermally activated manganese 1,4-benzenedicarboxylate metal organic framework with high anodic capability for Li-ion batteries, *New Journal of Chemistry*, 11(2016).
41. Zhang Y., Lin B., Sun Y., Zhang X., Yang H., Wang J., Carbon nanotubes@metal-organic frameworks as Mn-based symmetrical supercapacitor electrodes for enhanced charge storage, *RSC Adv.*, **5**, 58100-58106 (2015).
42. Sargazi G., Afzali D., Daldosso N., Kazemian H., Chauhan N.P., Sadeghian Z., Tajerian T., Ghafarinazari A., Mozafari M., A systematic study on the use of ultrasound energy for the synthesis of nickel-metal organic framework compounds, *Ultrason. Sonochem.* **27**, 395-402 (2015).
43. Yaghi O.M., Li H.L., Groy T.L., Construction of Porous Solids from Hydrogen-Bonded Metal Complexes of 1,3,5-Benzenetricarboxylic Acid, *J. Am. Chem. Soc.* **118**, 9096-9101 (1996).
44. Fu Y., Wang X.Y., Li G. B., Liao F. H., Xiong M., Lin J. H., Synthesis, structure and Magnetic property of Co(H₂BTC)₂(H₂O)₄(H₃BTC= Benzene 1,3,5-tricarboxylic acid. *Chinese J. Inorg. Chem.* **24**, 1224-1228 (2008).
45. He J. H., Zhang Y. T., Pan Q. H., Yu J. H., Ding H., Xu R. R., Three metal-organic frameworks prepared from mixed solvents of DMF and HAc, *Microporous and Mesoporous Materials* **90**, 145-152 (2006).
46. Chen J. X., Ohba M., Kitagawa S., Two New Coordination Polymers Based on Hexanuclear Metal Cluster Cores, *Chem. Lett.* **35**, 526-527 (2006).
47. Pauling L., The nature of the chemical bond. IV. The energy of single bonds and the relative electronegativity of atoms, *J. Am. Chem. Soc.*, **54** (9), 3570-3582 (1932).
48. Wu D., Yan W., Xu H., Zhang E., Li Q., Defect Engineering of Mn-based MOFs with Rod-shaped Building Units by Organic Linker Fragmentation, *Inorganica Chimica Acta* **460**, 93-98 (2017).
49. Coelho G. F., Gonçalves Jr A. C., Tarley C. R. T., Casarin J., Nacke H., Francziskowski M. A., Removal of metal ions Cd (II), Pb (II), and Cr (III) from water by the cashew nut shell Anacardium occidentale L, *Ecological Engineering* **73**, 514-525 (2014).

طريقه مبتكره لتحضير هياكل معدنيه عضويه تحتوي على معدن المنجنيز لإزاله أيونات الكاديوم والرصاص والزئبق من المياه

هويدا ممدوح عبد السلام^١، تامر ذكي^{٢،٣}

^١ قسم التحليل والتقييم بمعهد بحوث البترول – مدينة نصر - القاهرة - مصر.

^٢ قسم التكرير معمل الحفازات - معهد بحوث البترول –مدينة نصر- القاهرة - مصر.

^٣ معمل النانو تكنولوجى - معهد بحوث البترول –مدينة نصر - القاهرة - مصر.

هذا البحث يتضمن طريقة سهلة و سريعة لتحضير الهياكل المعدنية العضوية التي تحتوي على معدن المنجنيز باستخدام تقنيه موجات الميكروويف. يتم تقييم العينه المحضره من الهياكل المعدنية من خلال التحليل الحراري الوزني التفاضلي (TG-DTA، TA)، حيود الأشعة السينية (XRD)، تحليل مساحة السطح، قياس مدى الأشعه تحت الحمراء (FTIR) للمواد المحضره لوجود الرابطة الكيميائية، الميكروسكوب الإلكتروني النافذ (SEM).

دراسه كفاءه العينه المحضره من الهياكل المعدنية-العضويه نحو أيونات الكاديوم والرصاص والزئبق من المحاليل المائيه مع تطبيق النهج الحركية والديناميكا الحرارية. أوضحت نتائج البيانات كفاءة عالية اتجاه ادمصاص أيونات Cd، Pb، Hg من محلول مائي (٨١,٨٩٪، ٧١,١٩٪ و ٦٥,١٩٪ على التوالي). أن ادمصاص هذه الأيونات على الهياكل المعدنية-العضويه ذات صلته بمعدن المنجنيز تمت معالجتهم عن طريق آلية ملء المسام. تم التوصل على درجة الحموضة المثلى، الجرعة الممتازة، ودرجة الحرارة لتكون ٥، ١ غرام / لتر، و ٣٠ درجة مئوية، على التوالي.

تم إعادة استخدام Mn-MOF بنجاح حيث يوضح كفاءه العينه فى التجربه الاولى وكانت الكميات الممتازة لـ أيونات Cd، Pb، Hg (٨٠,٢٪، ٦٩,٦٪، ٦٤٪) وبعد التجربه الخامسة أصبح كفاءه العينه (٦٨٪، ٥٤,٧٤٪ و ٥٠,٩٨٪ على التوالي) وهذا توضيح قدرته على تطبيق ادمصاص هذه الأيونات الثقيلة من المياه.